

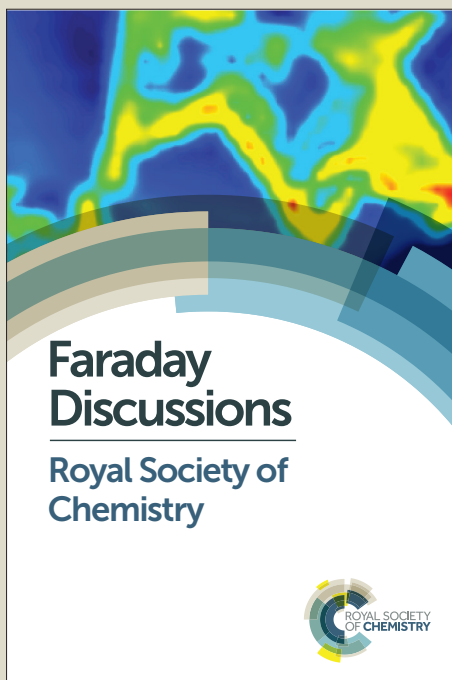
Faraday Discussions

Accepted Manuscript



This manuscript will be presented and discussed at a forthcoming Faraday Discussion meeting. All delegates can contribute to the discussion which will be included in the final volume.

Register now to attend! Full details of all upcoming meetings: <http://rsc.li/fd-upcoming-meetings>



This is an *Accepted Manuscript*, which has been through the Royal Society of Chemistry peer review process and has been accepted for publication.

Accepted Manuscripts are published online shortly after acceptance, before technical editing, formatting and proof reading. Using this free service, authors can make their results available to the community, in citable form, before we publish the edited article. We will replace this *Accepted Manuscript* with the edited and formatted *Advance Article* as soon as it is available.

You can find more information about *Accepted Manuscripts* in the [Information for Authors](#).

Please note that technical editing may introduce minor changes to the text and/or graphics, which may alter content. The journal's standard [Terms & Conditions](#) and the [Ethical guidelines](#) still apply. In no event shall the Royal Society of Chemistry be held responsible for any errors or omissions in this *Accepted Manuscript* or any consequences arising from the use of any information it contains.



Catalytic Dehydrogenation of Propane by Carbon Dioxide: A Medium-Temperature Thermochemical Process for Carbon Dioxide Utilisation

Received 00th January 20xx,
Accepted 00th January 20xx

DOI: 10.1039/x0xx00000x

www.rsc.org/

X. Du,^a B. Yao,^b S. Gonzalez-Cortes,^a V. L. Kuznetsov,^a Hamid AlMegren,^c T. Xiao,^{a*} P. P. Edwards,^{a*}

The dehydrogenation of C₃H₈ in the presence of CO₂ is an attractive catalytic route for C₃H₆ production. In studying the various possibilities to utilise CO₂ to convert hydrocarbons using the sustainable energy source of solar thermal energy, thermodynamic calculations were carried out for the dehydrogenation of C₃H₈ using CO₂ for the process operating in the temperature range of 300–500 °C. Importantly, the results highlight the enhanced potential of C₃H₈ as compared to its lighter and heavier homologues (C₂H₆ and C₄H₁₀, respectively). To be utilised in this CO₂ utilisation reaction the Gibbs Free Energy ($\Delta_r G_m^0$) of each reaction in the modelled, complete reacting system of the dehydrogenation of C₃H₈ in the presence of CO₂ also indicate that further cracking of C₃H₆ will affect the ultimate yield and selectivity of the final products. In a parallel experimental study, catalytic tests of the dehydrogenation of C₃H₈ in the presence of CO₂ over 5wt%–Cr₂O₃/ZrO₂ catalysts operating at 500 °C, atmospheric pressure, and for various C₃H₈ partial pressures and various overall GHSV (Gas Hourly Space Velocity) values. The results showed that an increase in the C₃H₈ partial pressure produced an inhibition of C₃H₈ conversion but, importantly, a promising enhancement of C₃H₆ selectivity. This phenomenon can be attributed to competitive adsorption on the catalyst between the generated C₃H₆ and inactivated C₃H₈, which inhibits any further cracking effect on C₃H₆ to produce by-products. As a comparison, the increase of the overall GHSV can also decrease the C₃H₈ conversion to a similar extent, but the further cracking of C₃H₆ cannot be limited.

1. Introduction

In an attempt to ameliorate the burgeoning growth in greenhouse gas emissions, there are currently intense efforts, world-wide, aimed at the utilisation of CO₂, particularly in its conversion to fuels and high-value chemical products^{1,2,3,4,5,6,7}. Chemical processes aimed at the utilisation and conversion of CO₂ are, of course, driven in a thermodynamic sense by the difference in Gibbs Free Energy between the resulting final chemical products, and CO₂ and the targeted reactants at the relevant experimental conditions. However CO₂ being a highly stable molecule will require a substantial amount of energy, effective catalysts and effective reaction conditions for any chemical conversion processes of CO₂ into fuels or high-value chemical products.

Thus probably all chemical reactions for CO₂ conversion and utilisation are endothermic and will consume considerable amounts of energy. If such energy is provided by fossil fuels, the net effect based on any well-to-wheels analysis of the process will invariably

result in a net production of CO₂; this situation could only be deemed beneficial from a climate mitigation perspective if the necessary input process energy is provided from renewable or sustainable sources.

The motivation behind this work, therefore, is to identify and develop specific chemical utilisation processes for CO₂ that can be achieved by the application of relatively easily-accessible solar thermal energy and associated thermochemical processes, using so-called "Low and Medium Temperature Thermochemical Processes", typically operating for temperature ranges of T ~250 °C and T ~250–500 °C, respectively.⁸

Utilising solar thermal energy at these lower temperatures for thermochemical processes than the widely-utilised High Temperature Process regime⁹ (T ~1000 °C) creates highly interesting and important challenges for catalysis science. Coupling and optimising the catalyst chemistry of CO₂ chemical reactions in the temperature/energy range of ca 300–500 °C with the engineering challenges of cheap, solar thermal collectors may allow the prospect of accessible, sustainable CO₂ utilisation. These coupled challenges therefore provide a high level of opportunity for modern catalysis science and engineering.

As an "improved" reaction of the dehydrogenation of C₃H₈, the dehydrogenation of C₃H₈ in the presence of CO₂ (C₃H₈ + CO₂ → C₃H₆ + H₂O + CO) has been heavily studied over the last decade.^{10,11,12,13,14,15} In this promising reaction, CO₂ acts as a mild oxidant to combine the dehydrogenation of C₃H₈ with a reverse

^a King Abdulaziz City of Science and Technology (KACST) - Oxford Centre of Excellence in Petrochemicals, Inorganic Chemistry Laboratory, Department of Chemistry, University of Oxford, Oxford, OX1 3QR, United Kingdom. E-mail: peter.edwards@chem.ox.ac.uk; Tel: +44(0)1865 272660; Fax: +44(0)1865 272690

^b SINOPEC Shanghai Petrochemical Company LTD., Shanghai, 200540, China

^c Petrochemicals Research Institute (PRI), King Abdulaziz City of Science and Technology (KACST), .Riyadh, Saudi Arabia, P.O. Box 6086, Riyadh 11442, Saudi Arabia

water gas shift ($\text{H}_2 + \text{CO}_2 \rightarrow \text{H}_2\text{O} + \text{CO}$), and hence, the equilibrium of the dehydrogenation of C_3H_8 can be shifted to the product side. Moreover, CO_2 may also reduce the coking effect of catalyst by coke gasification ($\text{C} + \text{CO}_2 \rightarrow 2\text{CO}$). Competitive adsorption among C_3H_8 , CO_2 and generated gaseous water can also explain the relatively lower initial conversion of C_3H_8 , the reduced coking effect, and higher stability of catalysts in the CO_2 atmosphere.^[16]

In this paper, the advantages of specifically selecting C_3H_8 as the feedstock for CO_2 utilisation are advanced for the lower temperature requirements, as compared to both its lighter and heavier alkane homologues, C_2H_6 and C_4H_{10} , respectively. Furthermore, in seeking the possibility to convert alkanes with the energy source from accessible solar heating technology, the temperature range to be targeted in thermodynamic calculations has been localised in the range 300-500°C which can be easily achieved, for example, by high pressure steam from a solar heating system.

The shift of the equilibrium state by CO_2 in the dehydrogenation of C_3H_8 has been identified from a thermodynamic analysis.^{17,18,19} However, the reaction systems modelled previously rarely take into consideration the competing side reactions and by-products. The dehydrogenation of C_3H_8 in the presence of CO_2 can be significantly affected by various competing side reactions which are deleterious to the targeted C_3H_6 yield, selectivity and indeed to the stability of the operating catalyst. Hence in this paper, the thermodynamic analysis was operated across a more comprehensive reaction system which covered all the possible by-products together with the generation of carbon—particularly important in a consideration of catalyst operating lifetimes

When considering the side reactions for the dehydrogenation of C_3H_8 in the presence of CO_2 , the major cause of by-products is the further cracking effect on C_3H_6 ,²⁰ and the competitive adsorption from CO_2 is claimed to be an effective way to inhibit that process.¹⁶ Our analysis reveals that the availability of active sites on the catalyst surface does indeed play a critical role in the reaction system. To observe the different performance properties of a catalyst when reactants are saturated, to the availability of active sites, the reactions were operated over a ZrO_2 -supported Cr_2O_3 catalyst with careful control of the various partial pressures of C_3H_8 but keeping a constant $\text{C}_3\text{H}_8/\text{CO}_2$ ratio. The reaction results exhibited high C_3H_6 selectivity by inhibiting the selectivity of by-products, which is promising result if these processes are to be applied in any larger, scale-up industrial process.

2. Thermodynamics and (selected) chemical reactions of carbon dioxide

In Figure 1 we illustrate the underlying thermodynamic considerations for the chemical utilisation of CO_2 , where the Gibbs free energy of formation of CO_2 and various related substances are shown for comparison. Any attempt at utilising CO_2 as a chemical reactant must therefore take account of the relative stability (Gibbs free energy) of the CO_2 utilisation reaction products, as compared to CO_2 and the other reactant(s)

Both contributing terms (ΔH and $T\Delta\text{S}$) for the Gibbs free energy are not favourable in converting CO_2 to other molecules. The carbon-oxygen bonds are strong and substantial energy is

needed for their dissociation and subsequent reduction. Similarly, the entropy term ($T\Delta\text{S}$) typically makes little or no contribution to the thermodynamic driving force for any CO_2 utilisation reaction.

The resulting Gibbs free energy of the CO_2 chemical utilisation reaction, ΔG , provides information as to the ultimate yield of reaction products at equilibrium, through the relationship $\Delta_r\text{G}_m^\ominus = -RT\ln(K^\ominus)$.

From Figure 2, however, the attractive option that the Gibbs free energy changes of CO_2 reaction becomes increasingly favourable by moving to higher members of the alkane homologous series. One notes, of course, that a ready solution for CO_2 utilisation is its conversion to the more reactive CO via the reverse water gas shift reaction ($\text{H}_2 + \text{CO}_2 \rightarrow \text{H}_2\text{O} + \text{CO}$), and subsequent use of syngas chemistry to yield the desired products. However, this attractive route clearly needs a ready source of H_2 and ideally a source of sustainable H_2 derived from non-fossil fuel routes. In the absence of hydrogen from low cost, low (zero) carbon sources, this process will yield a net CO_2 emission for the total wheel-to-wheel analysis.

Our research, then, looks in detail at the thermodynamics of the dehydrogenation of C_3H_8 by CO_2 as a potential prospect for CO_2 utilisation in temperature and reaction conditions where the ultimate application of solar thermal energy may be a promising technology. This is a specific example of the broader challenge facing any CO_2 utilisation technology; namely due to the inevitable input energy required to convert CO_2 to useful products, reducing CO_2 emissions through CO_2 utilisation will only be possible if the energy inputs are from renewable sources. We believe that Low-to-Medium Temperature Solar Thermochemical processes offer considerable opportunities in that regard and the research outlined here—setting out the complete thermodynamic analysis together with a catalytic chemistry study—may present a way forward for CO_2 utilisation

3. Thermodynamic calculations and simulations

3.1 Methods

In order to fully understand the thermodynamic basis of the dehydrogenation of C_3H_8 in the presence of CO_2 , in connecting also with the solar thermal technology which is normally set close to 500°C in the form of high pressure steam, the standard change of reaction in Gibbs free energy, $\Delta_r\text{G}_m^\ominus$, of the dehydrogenation of C_2 - C_4 alkanes with CO_2 utilisation ($\text{C}_n\text{H}_{2n+2} + \text{CO}_2 \rightarrow \text{C}_n\text{H}_{2n} + \text{H}_2\text{O} + \text{CO}$, $n = 2,3,4$) were calculated in the temperature range of 300-500°C. The cracking of C_1 - C_4 alkanes and olefins to form carbon ($\text{C}_n\text{H}_m \rightarrow n\text{C} + \frac{m}{2}\text{H}_2$, $n = 1,2,3,4$) were also included in these calculations in this temperature range to indicate the potential coking ability on operating catalysts of each substances.

Here, $\Delta_r\text{G}_m^\ominus$ of each single reaction in the temperature range of 300-500°C was calculated as following:

$$\textcircled{1}, \Delta_r\text{H}_m^\ominus(298.15\text{K}) = \sum_j v_j \Delta_r\text{H}_m^\ominus(298.15\text{K}, j)$$

$$\textcircled{2}, \Delta_r\text{H}_m^\ominus(T) = \Delta_r\text{H}_m^\ominus(298.15\text{K}) + \sum_j v_j \int_{298.15}^T C_{p,m} dT$$

$$\textcircled{3}, \Delta_r\text{S}_m^\ominus(298.15\text{K}) = \sum_B v_B \text{S}_m^\ominus(298.15\text{K})$$

$$\textcircled{4}, \Delta_r\text{S}_m^\ominus(T) = \Delta_r\text{S}_m^\ominus(298.15\text{K}) + \sum_j v_j \int_{298.15}^T \frac{C_{p,m}}{T} dT$$

$$\textcircled{5}, \Delta_r G_m^\ominus = \Delta_r H_m^\ominus - T \Delta_r S_m^\ominus$$

In the functions above, $\Delta_r H_m^\ominus$ is the standard molar enthalpy of formation, S_m^\ominus is the standard molar entropy, while $C_{p,m}$ is the parameters of molar heat capacity at constant pressure. The property parameters can be looked up from the chemical properties hand books, and these parameters of the related substances are list in Table 1 below.

3.2 Thermodynamic advantages of the dehydrogenation of C₃H₈ in the presence of CO₂

Figure 3 exhibits the standard change of reaction in Gibbs free energy ($\Delta_r G_m^\ominus$) of the reactions being compared. In the temperature range of 300-500°C, all dehydrogenation reactions show a similar trend. The highest $\Delta_r G_m^\ominus$ is found for the process to dehydrogenate C₂H₆ with CO₂ indicating that it is much harder to operate this reaction as compared to other low-n alkanes at 300-500°C. Importantly, $\Delta_r G_m^\ominus$ does not keep falling as the carbon number of alkane increases, and to dehydrogenate C₃H₈ with CO₂ appears more feasible than some C₄ reactions, for example

The $\Delta_r G_m^\ominus$ of alkane and olefin cracking to generate carbon and H₂ are shown in Figure 4, The C₄ alkanes have multiple curves because of their constituent isomers. In general, the lower the value of $\Delta_r G_m^\ominus$ indicates a higher possibility of cracking. Hence, the olefins show much higher cracking possibility than any alkanes, which imply that the selectivity of target products will be greatly affected by further cracking of olefins. For instance, C₃H₆ will be further cracked to lower level hydrocarbons or even carbon, so the selectivity will be reduced. It is also obvious that CH₄ has the highest resistance to coking, and as a sequence of stepwise mechanism of hydrocarbon decomposition, it will be a major by-product in these reaction systems when looking at olefins only, it is obvious that the carbon number is the most important indicator of the cracking possibility. With the similar $\Delta_r G_m^\ominus$ of dehydrogenation of alkane with CO₂, C₃H₆ has much higher resistance to cracking than any isomers of butene. Although C₂H₄ has even higher resistance to subsequent cracking, it is even more difficult for C₂H₆ to be activated with CO₂ when the temperature is kept below 500°C. From this analysis, the dehydrogenation of C₃H₈ in the presence of CO₂ is recognisably the best alkane to be targeted for a chemical utilisation process for CO₂ operating in this temperature range, a range specifically chosen for ready-availability of solar heating technology for these conditions

3.3 Modelled calculations of the dehydrogenation of C₃H₈ in the presence of CO₂

In reality, of course, the dehydrogenation of C₃H₈ in the presence of CO₂ is not a simple single reaction but a multiple reaction system, as shown in Table 2, mainly coupling the traditional dehydrogenation of C₃H₈ (reaction 1) and reverse water gas shift (reaction 2).

In this system, (1) and (2) are the main reactions considered; (3) and (4) are further cracking of C₃ species where lighter by-products are formed; (5) is the reaction to gasify the carbon deposition.

The $\Delta_r G_m^\ominus$ of reaction (1), (2), (3) and (5) are shown in Figure 5, while the ones of hydrocarbons cracking (reaction 4) are already displayed in Figure 4. From 300-500°C, only the cracking of C₂ and C₃, including reaction (3), can reach to a negative value of $\Delta_r G_m^\ominus$, which means these reactions are thermodynamically favoured. On

the contrary, the decomposition of CH₄ is not favoured in this temperature range. Considering C₃H₈ is the feedstock in this system and the stepwise mechanism of hydrocarbons to be decomposed, the generation of CH₄ can be an important indicator to measure the degree, and extent of side reactions during the reaction process. CO₂, as a mild oxidant, is not favoured to gasify the formed carbon deposition. Hence, CO₂ is always applied in order to shift the equilibrium without increasing the temperature. It is obvious that all other reactions in this system depend strongly on the conversion of C₃H₈ in reaction (1). Thus, when considering only reaction (1), this is a decomposition reaction which is favoured under lower partial pressure of C₃H₈. With the equilibrium constants calculated from $\Delta_r G_m^\ominus$ at the temperature range of 300-500°C, the conversions of C₃H₈ under different partial pressure is calculated as shown in Figure 6.

$$K^\ominus = \exp \left[\frac{-\Delta_r G_m^\ominus}{RT} \right]$$

The C₃H₈ conversion is observed to be significantly affected by the partial pressure of C₃H₈ within the temperature range of 300-500°C, it is for this reason that the dehydrogenation of C₃H₈ in the presence of CO₂ should be operated with very low partial pressure of C₃H₈ when designing experiments.

Apart from the improvement of catalysts, higher C₃H₆ selectivity can also be achieved by changing the conditions of reaction. A general way to inhibit the reaction extent is to limit the contact time of reactants on a catalyst surface by increasing the space velocity of gas flow.²¹ As a comparison we model this and also increase the partial pressure of reactants operating under these conditions.

4. Experimental

4.1 Catalyst preparation

To prepare the 5wt% of Cr₂O₃/ZrO₂ catalyst by precipitation method, ZrO₂ (Alfa-Aesor, 90m²/g, 99%) was pre-heated at 600 for 6 hour before being grinded and sieved to <125µm in particle size. Then, Cr(NO₃)₃·9H₂O precursor (99%, Sigma Aldrich) was dissolved into distilled water, and this solution was mixed with the ground ZrO₂ support and stirred at room temperature for 24 hours. To achieve Cr₂O₃-ZrO₂, the as prepared suspension was dried to obtain a slurry or paste, which was finally calcined at 600°C for 6 hours in a muffle furnace using a heating ramp of 10 °C/min. The solid sample was ground to obtain fine particles <125µm.

4.2 Catalyst Characterisation

All the samples, including ZrO₂ support, were characterized with high resolution X-ray Diffraction (XRD) using a PANalytical X'Pert PRO diffractometer with CuKα radiation (45kV, 40mA). When being scanned, samples were flat loaded in the custom-built sample holders and scanned from 20° to 30° 2θ with a step size of 0.0084° and a scanning speed at 0.017778° s⁻¹.

The amount of carbon deposition on the spent catalyst was measured via the thermo gravimetric analysis (TGA). The instrument employed was a TA Instrument, SDT Q-600, using flowing air at 100ml/min from 50°C to 1000°C with a ramp rate of 10°C/min. The TGA curves were also derived as D-TGA to show the rate of weight losses of samples

4.3 Catalyst Testing

The stability test of C₃H₈ dehydrogenation in the presence of CO₂ was operated in an M-R-10A micro-reactor (KUNLUN YONGTAI Company, China) over the Cr-based catalyst prepared as above. All tests were operated under atmospheric pressure and 500 °C for 5 hours, and the C₃H₈/CO₂ mixture, whose mole ratio was kept at C₃H₈/CO₂=1:2. As shown in Table 3, the conditions of tests differed from each other by two variables, the mole fractions of C₃H₈ (and CO₂) and overall gas hourly space velocity (GHSV). N₂ balance was applied to dilute the gas mixture. Considering that the reactions were operated under atmospheric pressure, the partial pressure of C₃H₈ in "R-4800x2" and "R-4800x3" was increased, and the GHSV of C₃H₈ was changed to the same level as "R-9600" and "R-14400" respectively.

The composition of outlet gas was tested by an online Gas Chromatography (PerkinElmer, Clarus 580 GC), and the conversions of C₃H₈ and CO₂, the selectivity of products, and the carbon balance in gaseous products can be determined with the following equations:

$$\text{Conversion}(\%) = C_i = 1 - \frac{x_i^{\text{outlet}} \cdot x_{N_2}^{\text{inlet}}}{x_i^{\text{inlet}} \cdot x_{N_2}^{\text{outlet}}} \times 100 \quad (i = \text{C}_3\text{H}_8 \text{ or } \text{CO}_2)$$

$$\text{Flow of gas in product (ml/min)} = F_j^{\text{outlet}} = \frac{X_j^{\text{outlet}} \cdot \text{flow of N}_2}{X_{N_2}^{\text{outlet}}}$$

$$(j = \text{H}_2, \text{CO}, \text{CO}_2, \text{CH}_4, \text{C}_2\text{H}_4, \text{C}_2\text{H}_6, \text{C}_3\text{H}_6, \text{C}_3\text{H}_8)$$

$$\text{Selectivity of Hydrocarbon}(\%) = S_{\text{C}_n\text{H}_m} = \frac{n \times F_{\text{C}_n\text{H}_m}^{\text{outlet}}}{3 \times F_{\text{C}_3\text{H}_8}^{\text{inlet}} \times C_{\text{C}_3\text{H}_8}} \times 100$$

$$\text{Yield of CO}(\%) = Y_{\text{CO}} = \frac{F_{\text{CO}}^{\text{outlet}}}{2 \times F_{\text{CO}_2}^{\text{inlet}}} \times 100$$

$$\text{Carbon Balance}(\%) = B_C = \frac{F_{\text{CH}_4}^{\text{outlet}} + 2 \times F_{\text{C}_2\text{H}_4}^{\text{outlet}} + 2 \times F_{\text{C}_2\text{H}_6}^{\text{outlet}} + 3 \times F_{\text{C}_3\text{H}_6}^{\text{outlet}} + 3 \times F_{\text{C}_3\text{H}_8}^{\text{outlet}} + F_{\text{CO}}^{\text{outlet}} + F_{\text{CO}_2}^{\text{outlet}}}{3 \times F_{\text{C}_3\text{H}_8}^{\text{inlet}} + F_{\text{CO}_2}^{\text{inlet}}} \times 100$$

$$\text{Oxygen Balance}(\%) = B_O = \frac{2 \times F_{\text{CO}_2}^{\text{outlet}} + F_{\text{CO}}^{\text{outlet}}}{2 \times F_{\text{CO}_2}^{\text{inlet}}} \times 100$$

5. Results and Discussion

5.1 Catalytic test results

The C₃H₈ conversion and C₃H₆ selectivity of the reaction under different C₃H₈ partial pressures and overall GHSV are shown in Figure 7. The results reveal effective C₃H₈ conversions at each specified condition while the C₃H₆ selectivity drops at the beginning of reactions. The results with different mole fractions of C₃H₈ were displayed with solid symbols and the conclusion drawn from the data in these figures is an inhibition of C₃H₈ conversion, but also an improvement in C₃H₆ selectivity. However, with the same increase of C₃H₈ fractional GHSV (by increasing the overall GHSV), the C₃H₈ conversion was inhibited to a similar extent while the C₃H₆ selectivity decreased also. These comparative results indicate that even though the C₃H₈ conversion was similarly inhibited via the two routes to increase the C₃H₈ fractional GHSV, the underpinning mechanisms were fundamentally different.

Figure 8 exhibits the production of CH₄, the main by-product. The initial selectivity of CH₄ was decreased from 6% to 3% as an increase of C₃H₈ fractional GHSV. The CH₄ selectivity can roughly indicate the cracking capability of catalyst on higher level

hydrocarbons, which indirectly exhibits the extent of further cracking effect on C₃H₆ during the reaction.

5.2 Discussion on the changes of C₃H₆ selectivity.

The conversion of reactants and the mass balances of carbon and oxygen elements are shown in Table 4. In contrast to the high stability of the C₃H₈ conversion, the CO₂ conversions dropped drastically over the first 5 hours. This may be due to the various and different sites for C₃H₈ and CO₂ to be adsorbed on the catalyst surface respectively; C₃H₈ is usually attached to Cr species while CO₂ can be adsorbed at the interface between Cr₂O₃ dopant and ZrO₂ support.²² The high level of C-Balance indicates the low generation of solid and liquid C-containing product; this confirms the high stability of C₃H₈ conversions in each test. The O-balance, which was higher than 100% at the end of the test, indicates additional, extraneous oxygen must have entered into the gaseous phase during the reaction, and the oxygen source can be attributed to the reduction of high valence state chromium species (Cr⁶⁺/Cr⁵⁺) on the catalyst surface.²³ Weckhuysen et al.²⁴ claimed that Cr⁶⁺ plays as a precursor for the Cr dehydrogenation centres, and the reduction of Cr species is assumed to be one of the primary deactivation mechanisms.

Table 5 is a compilation of the selectivity of gaseous products. The reduced level of C₂H_x production as compared to that of the selectivity of CH₄ was observed). This experimental trend matched the prediction (highlighted in Figure 4) that CH₄ is much more difficult to be thermally cracked at 500 °C than corresponding C₂ molecules. The decrease of CO yield was not as much as the trend of CO₂ conversion; we believe this is due to the carbon gasification by reducing the chromium species (Cr⁶⁺/Cr⁵⁺) on catalyst surface, which matches the observed increasing O-balance.

The XRD patterns of 5wt%-Cr₂O₃/ZrO₂ before and after the catalytic tests are displayed in Figure 9, and the pattern of the ZrO₂ support is also shown here as reference. The peak at 2θ=36.18° is corresponds to the 1-1-0 phase of Cr₂O₃ with rhombohedral crystal symmetry. No peak shift or new peaks were observed from the post-reaction catalyst, which indicated that no phase change occurred during the catalytic test. Importantly, this also matched the high stability of C₃H₈ conversions, as shown in Figure 7.

Thermo gravimetric analysis (TGA) results and the corresponding derivative weight -to - temperature (D-TGA) plots are displayed in Figure 10. The weight loss starting from 200 °C we attribute to the combustion of amorphous carbon in air. The integrated area of the derivative weight equals to the weight loss, which displayed more coke formed with an increase of the C₃H₈ fractional GHSV.

In general terms, the mechanism of C₃H₈ dehydrogenation in the presence of CO₂ involves the primary activation of C₃H₈ on the catalyst surface, while CO₂ provides a contribution to the reaction equilibrium shift by oxidising H₂ generated from the C₃H₈ dehydrogenation (via the reverse water gas shift reaction, H₂ + CO₂ → H₂O + CO). From the macro perspective, the average contact time for each C₃H₈ molecule is shortened with the higher C₃H₈ fractional GHSV, and this is the cause of a decreased C₃H₈ conversion by optimising both methods to modify the C₃H₈ fractional GHSV. However, the observed changes of C₃H₆ selectivity indicate that only increasing the partial pressure of reactants can effectively inhibit the further cracking of C₃H₆. This arises because the competitive adsorption between C₃H₆ and other substances are strengthened from the micro perspective

Conclusions

With the aim of attempting to (ultimately) correlate the dehydrogenation of C_3H_8 in the presence of CO_2 with the energy source from solar heating technology, thermodynamic calculations were operated for chemical processes operating in the temperature range 300-500 °C. An important outcome is the great potential of C_3H_8 as compared to its lighter and heavier homologues (C_2H_6 and C_4H_{10} , respectively) from both the perspective of CO_2 activation and also coking resistance across this temperature range. The $\Delta_r G_m^\ominus$ of each reaction in our thermodynamic modelling of the dehydrogenation of C_3H_8 in the presence of CO_2 also indicated that neither the reverse water gas shift nor the coke gasification with CO_2 are favoured at 300-500

A series of catalytic tests were carried out over 5wt%- Cr_2O_3/ZrO_2 at various C_3H_8 partial pressure and overall GHSV. It was shown that the increase of C_3H_8 partial pressure is highly beneficial for the enhancement of C_3H_6 selectivity. Meanwhile, the C_3H_8 conversion was sacrificed due to the competitive adsorption between the produced C_3H_6 and inactivated C_3H_8 molecules, which was the major reason for the inhibition of further cracking of C_3H_6 . As a comparison, the increase of the overall GHSV can also decrease the C_3H_8 conversion to the similar extent. However, the further cracking of C_3H_6 cannot be limited because only the contacting time of C_3H_8 on the catalyst surface was shortened from this micro perspective.

From the aspect of the ultimate application of this particular CO_2 utilisation processes, we believe that the enhancement of selectivity of the (target) C_3H_6 product, whilst sacrificing some of the reactants' ultimate conversion is acceptable. The efficiency can be improved by a cycle system involving the reuse of the unconverted feedstock by separating from the outlet mixture and subsequently cycling back to the inlet mixture. It is recognised that this kind of cycle system is beneficial to the reactions with low conversion but very high selectivity. The high thermo-stability of the present catalyst makes it attractive to scale-up to a moving bed or even a fluid bed reactor for catalyst regeneration.

We believe that the results presented here are promising in terms of the underpinning catalyst science for establishing the potential industrialisation of the process of CO_2 utilisation through C_3H_8 dehydrogenation. This type of CO_2 utilisation, operating in the relatively low temperature range of 300-500 – and easily accessible by solar thermochemical routes, could help shift the focus of CO_2 interest from the disposal of an inconvenient by-product – typified by the process of Carbon Capture and Storage (CCS) – towards the production and use of CO_2 as a commodity chemical in Carbon Capture and Utilisation (CCU). However, one must stress again that any proposed CCU process to be realistic for emission reduction potential can only be beneficial if any necessary energy input is from renewable sources. As noted here, our view is that solar thermal chemical processes for CO_2 utilisation, accessible across these temperature ranges, offer very considerable potential in that important regard.

Acknowledgements

We thank the China Scholarship Council (CSC) for financial support to X. Du and KACST and EPSRC for their continued support.

References

1. C. Song, *Catal. Today*, 2006, **115**, 2-32.
2. F. Schierbaum, *Carbon dioxide as chemical feedstock. Edited by Michele Aresta*, 2010.
3. Z. Jiang, T. Xiao, V. L. Kuznetsov and P. P. Edwards, *Philos. Trans. R. Soc., A*, 2010, **368**, 3343-3364.
4. F. T. Zangeneh, S. Sahebdehfar and M. T. Ravanchi, *J. Nat. Gas Chem.*, 2011, **20**, 219-231.
5. S. J. Bennett, D. J. Schroeder and S. T. McCoy, *Energy Procedia*, 2014, **63**, 7976-7992.
6. presented in part at the ADP technical Expert meetings, **Bonn, Germany**, 2014.
7. C. Ampelli, S. Perathoner and G. Centi, *Philos. Trans. R. Soc., A*, 2015, **373**, 1-35.
8. P. Phelan, T. Otanicar, R. Taylor and H. Tyagi, *J. Therm. Sci. Eng. Appl.*, 2013, **5**, 021003/021001-021003/021009.
9. G. Maag, G. Zanganeh and A. Steinfeld, *Int. J. Hydrogen Energy*, 2009, **34**, 7676-7685.
10. D. B. Fox, E. H. Lee and M.-H. Rei, *Ind. Eng. Chem., Prod. Res. Develop.*, 1972, **11**, 444-446.
11. P. Michorczyk and J. Ogonowski, *React. Kinet. Catal. Lett.*, 2003, **78**, 41-47.
12. K. Takehira, Y. Ohishi, T. Shishido, T. Kawabata, K. Takaki, Q. Zhang and Y. Wang, *J. Catal.*, 2004, **224**, 404-416.
13. A. L. Lapidus, N. A. Gaidai, Y. A. Agafonov, N. V. Nekrasov, D. V. Trushin, A. V. Makashov, M. A. Botavina, G. Martra and S. Coluccia, *DGMK Tagungsber.*, 2008, **2008-3**, 275-282.
14. M. Chen, J.-L. Wu, Y.-M. Liu, Y. Cao, L. Guo, H.-Y. He and K.-N. Fan, *Appl. Catal., A*, 2011, **407**, 20-28.
15. P. Michorczyk, P. Kustrowski, A. Kolak and M. Zimowska, *Catal. Commun.*, 2013, **35**, 95-100.
16. T. Shishido, K. Shimamura, K. Teramura and T. Tanaka, *Catal. Today*, 2012, **185**, 151-156.
17. L. Liu, H. Liu, C.-y. Li and S.-f. Ji, *Beijing Huagong Daxue Xuebao, Ziran Kexueban*, 2005, **32**, 9-13.
18. R. Shangguan, X. Ge, J. Wang and J. Shen, *Shiyou Yu Tianranqi Huagong*, 2002, **31**, 5-7.
19. K. Mueller, A. Baumgaertner, L. Mokrushina and W. Arlt, *Chem. Eng. Technol.*, 2014, **37**, 1261-1264.
20. F. Solymosi and P. Tolmascov, *Catal. Lett.*, 2002, **83**, 183-186.
21. H. Liu, Z. Zhang, H. Li and Q. Huang, *J. Nat. Gas Chem.*, 2011, **20**, 311-317.
22. S. Naito, M. Tsuji and T. Miyao, *Catal. Today*, 2002, **77**, 161-165.
23. S. Deng, S. Li, H. Li and Y. Zhang, *Ind. Eng. Chem. Res.*, 2009, **48**, 7561-7566.
24. B. M. Weckhuysen and R. A. Schoonheydt, *Catal. Today*, 1999, **51**, 223-232.

**Catalytic Dehydrogenation of Propane by Carbon Dioxide: A
Medium-Temperature Thermochemical Process for Carbon Dioxide
Utilisation**

X. Du,^a B. Yao,^b S. Gonzalez-Cortes,^a V. L. Kuznetsov,^a Hamid AlMegren,^c T. Xiao,^{a*} P. P. Edwards,^{a*}

^a, King Abdulaziz City of Science and Technology (KACST) - Oxford Centre of Excellence in Petrochemicals, Inorganic Chemistry Laboratory, Department of Chemistry, University of Oxford, Oxford, OX1 3QR, United Kingdom.

^b, SINOPEC Shanghai Petrochemical Company LTD., Shanghai, 200540, China

^c, Petrochemicals Research Institute (PRI), King Abdulaziz City of Science and Technology (KACST), Riyadh, Saudi Arabia, P.O. Box 6086, Riyadh 11442, Saudi Arabia

* Corresponding Author.

P. P Edwards, Tel: +44(0)1865 272646; Fax: +44(0)1865 272656;

E-mail address: peter.edwards@chem.ox.ac.uk.

T. Xiao, Tel: +44(0)1865 272660; Fax: +44(0)1865 272690

E-mail address: xiao.tiancun@chem.ox.ac.uk

Table 1: Standard thermodynamic properties of chemical substance:
Standard molar enthalpy of formation($\Delta_f H_m^\theta$)¹, standard molar entropy(S_m^θ)¹ and parameters
of molar heat capacity at constant pressure($C_{p,m}$)².

Substance	$\Delta_f H_m^\theta(298.15K)$ (K J mol ⁻¹)	$S_m^\theta(298.15K)$ (J K ⁻¹ mol ⁻¹)	$C_{p,m} = A + BT + CT^2 + DT^3 + ET^4$				
			A($\times 10^0$)	B($\times 10^{-3}$)	C($\times 10^{-5}$)	D($\times 10^{-8}$)	E($\times 10^{-11}$)
H ₂	0	130.684	2.883	3.681	-0.772	0.692	-0.213
CO	-110.53	197.67	3.912	-3.913	1.182	-1.302	0.515
CO ₂	-393.51	213.74	3.259	1.356	1.502	-2.374	1.056
H ₂ O	-241.82	188.83	4.395	-4.186	1.405	-1.564	0.632
CH ₄	-74.81	186.26	4.568	-8.975	3.631	-3.407	1.091
C ₂ H ₄	52.26	219.56	4.221	-8.782	5.795	-6.729	2.511
C ₂ H ₆	-84.68	229.6	4.178	-4.427	5.660	-6.651	2.487
C ₃ H ₆	20.42	267.05	3.834	3.893	4.688	-6.013	2.283
C ₃ H ₈	-103.85	269.91	3.847	5.131	6.011	-7.893	3.079
1-C ₄ H ₈	-0.13	305.71	4.389	7.984	6.143	-8.197	3.165
cis-2-C ₄ H ₈	-6.99	300.94	3.689	19.184	2.230	-3.426	1.256
trans-2-C ₄ H ₈	-11.17	296.59	5.584	-4.890	9.133	-10.975	4.085
i-C ₄ H ₈	-17.10	295.29	3.231	20.949	2.313	-3.949	1.566
n-C ₄ H ₁₀	-126.15	310.23	5.547	5.536	8.057	-10.571	4.134
i-C ₄ H ₁₀	-134.73	291.82	3.351	17.883	5.477	-8.099	3.243
C (graphite)*	0	5.74	-0.977	9.458	-1.118	0.739	-0.207

*: The parameters of $C_{p,m}$ are calculated by regressing the molar heat capacity at various temperature in handbook.³

Table 2. Modelled reaction system for the dehydrogenation of C₃H₈ in the presence of CO₂

Reaction Number	Reaction Formula
(1)	$C_3H_8 \rightarrow C_3H_6 + H_2$
(2)	$H_2 + CO_2 \rightarrow H_2O + CO$
(3)	$C_3H_8 \rightarrow C_2H_4 + CH_4$
(4)	$C_nH_m \rightarrow nC + \frac{m}{2}H_2$
(5)	$C + CO_2 \rightarrow 2CO$

Table 3. Mole fractions of C₃H₈ ($X_{C_3H_8}$), overall GHSV and C₃H₈ GHSV of the coded reactions

Reaction code	$X_{C_3H_8}$ (mol%)	GHSV (ml h ⁻¹ g _{cat} ⁻¹)	GHSV of C ₃ H ₈ (ml h ⁻¹ g _{cat} ⁻¹)
R-4800	5	4800	240
R-4800x2	10	4800	480
R-4800x3	15	4800	720
R-9600	5	9600	480
R-14400	5	14400	720

Table 4. Conversion of reactants ($C_{C_3H_8}$, C_{CO_2}) and balance of elements (B_C , B_O , B_H) in gaseous products over 5wt%-Cr₂O₃/ZrO₂ at various C₃H₈ partial pressure and overall GHSV; 500 °C and C₃H₈/CO₂ = 0.5.

C ₃ H ₈ Partial Pressure (atm)	C _{C₃H₈} (%)		C _{CO₂} (%)		B _C (%)		B _O (%)	
	0h	5h	0h	5h	0h	5h	0h	5h
R-4800	15.09	16.37	6.95	1.80	99.27	99.17	96.64	103.80
R-4800x2	9.52	11.03	4.62	2.79	99.90	99.30	97.80	103.16
R-4800x3	8.28	8.05	3.29	1.78	99.99	99.91	99.04	101.45
R-9600	9.77	10.35	5.15	1.51	98.65	98.87	96.93	102.42
R-14400	9.57	10.00	4.50	1.19	98.55	98.80	97.30	101.78

Table 5. Yield of CO (Y_{CO}) and Selectivity of hydrocarbons (S_i) over 5wt%-Cr₂O₃/ZrO₂ at various C₃H₈ partial pressure and overall GHSV; 500 °C and C₃H₈/CO₂ = 0.5.

C ₃ H ₈ Partial Pressure (atm)	Y _{CO} (%)		S _{CH₄} (%)		S _{C₂H_x} (%)		S _{C₃H₆} (%)	
	0h	5h	0h	5h	0h	5h	0h	5h
R-4800	3.59	3.54	6.06	3.76	1.32	1.00	83.23	64.30
R-4800x2	2.43	2.42	5.07	3.13	1.52	1.36	92.75	72.47
R-4800x3	1.94	1.89	4.74	2.48	1.66	1.88	94.56	80.30
R-9600	2.08	1.80	5.17	2.88	1.50	1.33	76.81	62.31
R-14400	1.80	1.57	3.26	1.68	1.46	1.35	75.91	61.53

References

1. P. Atkins and J. de Paula, *Atkins' Physical Chemistry, 7th Edition*, 2002.
2. J. Kunesh, *The Properties of Gases and Liquids, Fifth Edition* by Bruce Poling, John Prausnitz and John O'Connell, 2002.
3. W. M. Haynes, *CRC Handbook of Chemistry and Physics on DVD, Version 2012*, 2011.

**Catalytic Dehydrogenation of Propane by Carbon Dioxide: A
Medium-Temperature Thermochemical Process for Carbon Dioxide
Utilisation**

X. Du,^a B. Yao,^b S. Gonzalez-Cortes,^a V. L. Kuznetsov,^a Hamid AlMegren,^c T. Xiao,^{a*} P. P. Edwards,^{a*}

^a, King Abdulaziz City of Science and Technology (KACST) - Oxford Centre of Excellence in Petrochemicals, Inorganic Chemistry Laboratory, Department of Chemistry, University of Oxford, Oxford, OX1 3QR, United Kingdom.

^b, SINOPEC Shanghai Petrochemical Company LTD., Shanghai, 200540, China

^c, Petrochemicals Research Institute (PRI), King Abdulaziz City of Science and Technology (KACST), Riyadh, Saudi Arabia, P.O. Box 6086, Riyadh 11442, Saudi Arabia

* Corresponding Author.

P. P Edwards, Tel: +44(0)1865 272646; Fax: +44(0)1865 272656;

E-mail address: peter.edwards@chem.ox.ac.uk.

T. Xiao, Tel: +44(0)1865 272660; Fax: +44(0)1865 272690

E-mail address: xiao.tiancun@chem.ox.ac.uk

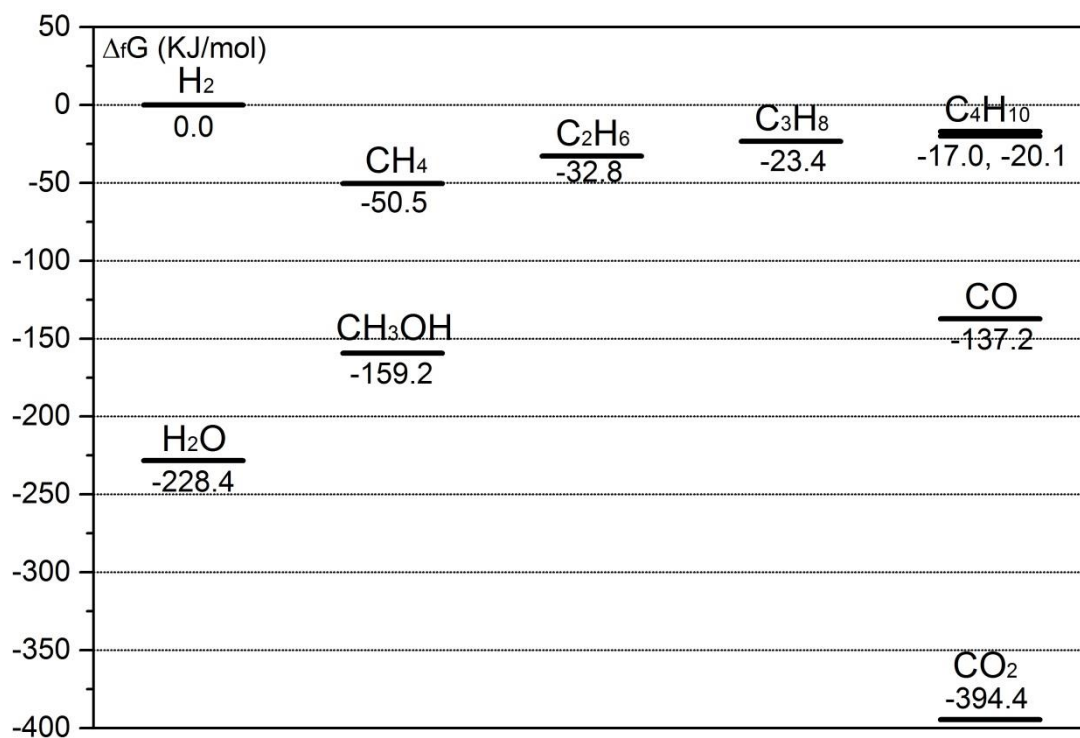


Figure 1 $\Delta_r G_m^\ominus$ of CO_2 and related substances at normal temperature and pressure (NTP).

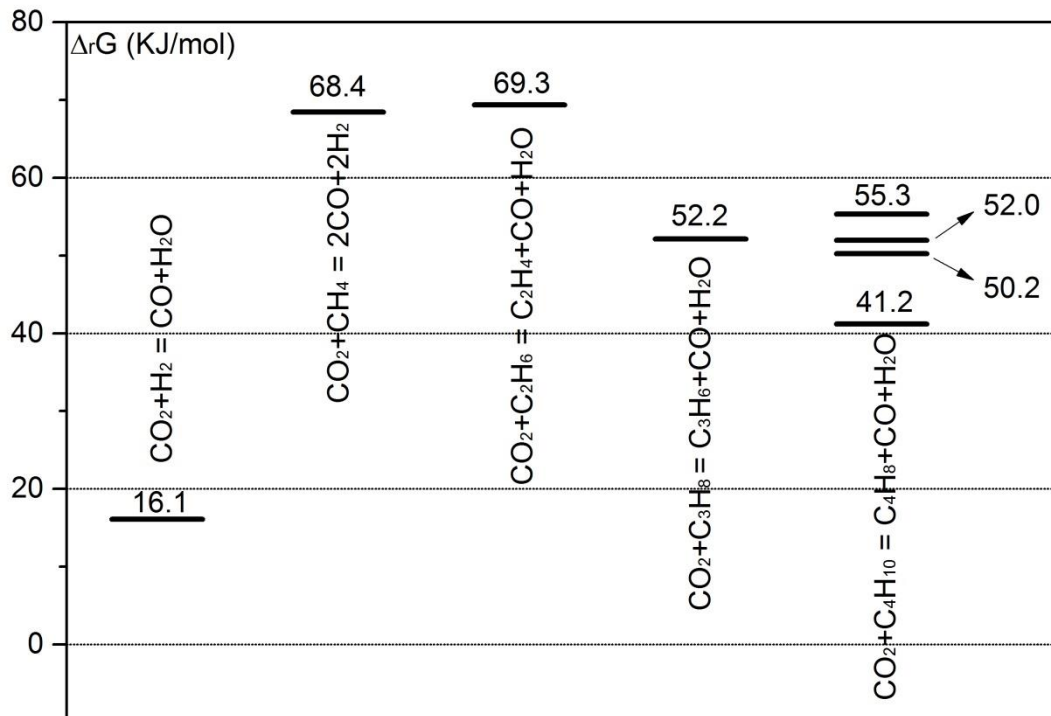


Figure 2 $\Delta_r G_m^\ominus$ of the reactions between CO_2 and other substances at 400°C and normal pressure.

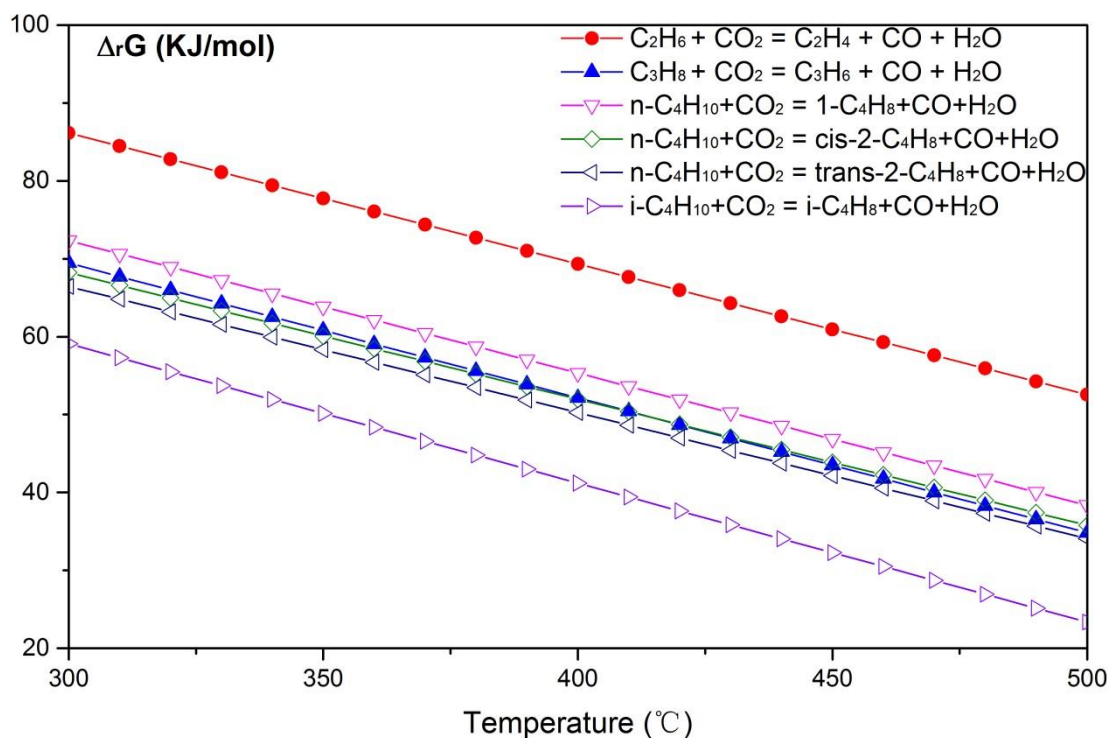


Figure 3 $\Delta_r G_m^\theta$ of the dehydration of light alkane in the presence of CO_2 at 300-500°C.

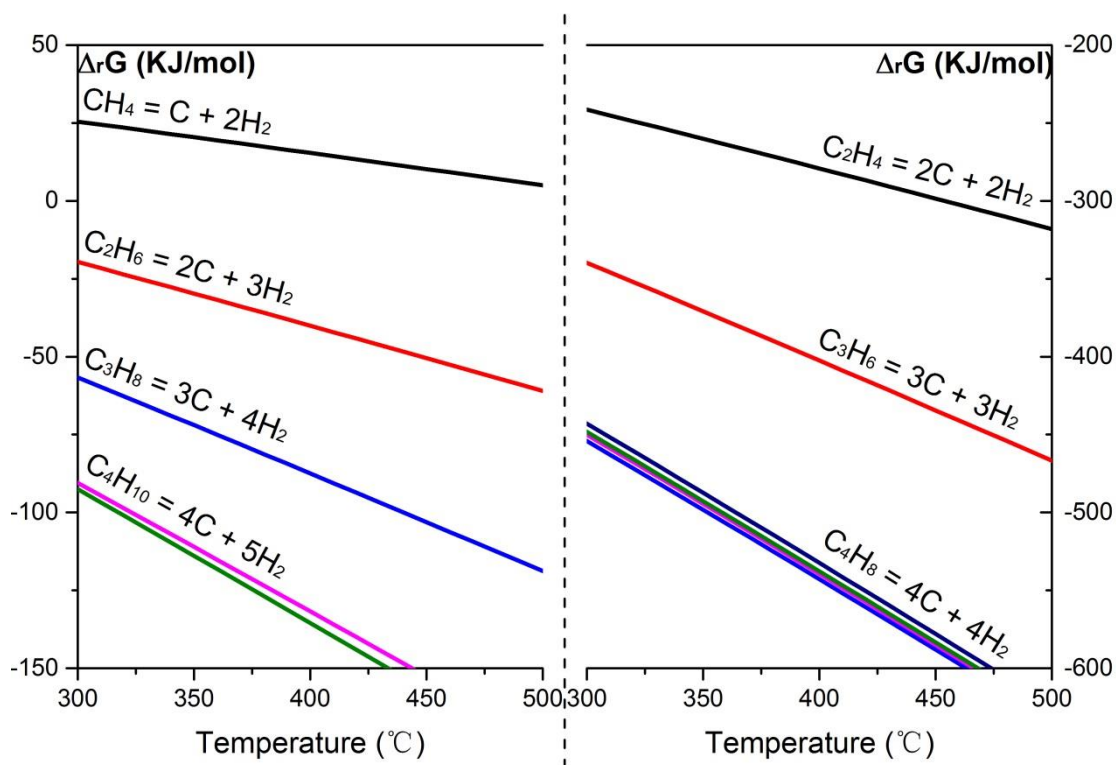


Figure 4 $\Delta_r G_m^\theta$ of the alkanes (left) and olefins (right) cracking to generate carbon and H_2 at 300-500°C.

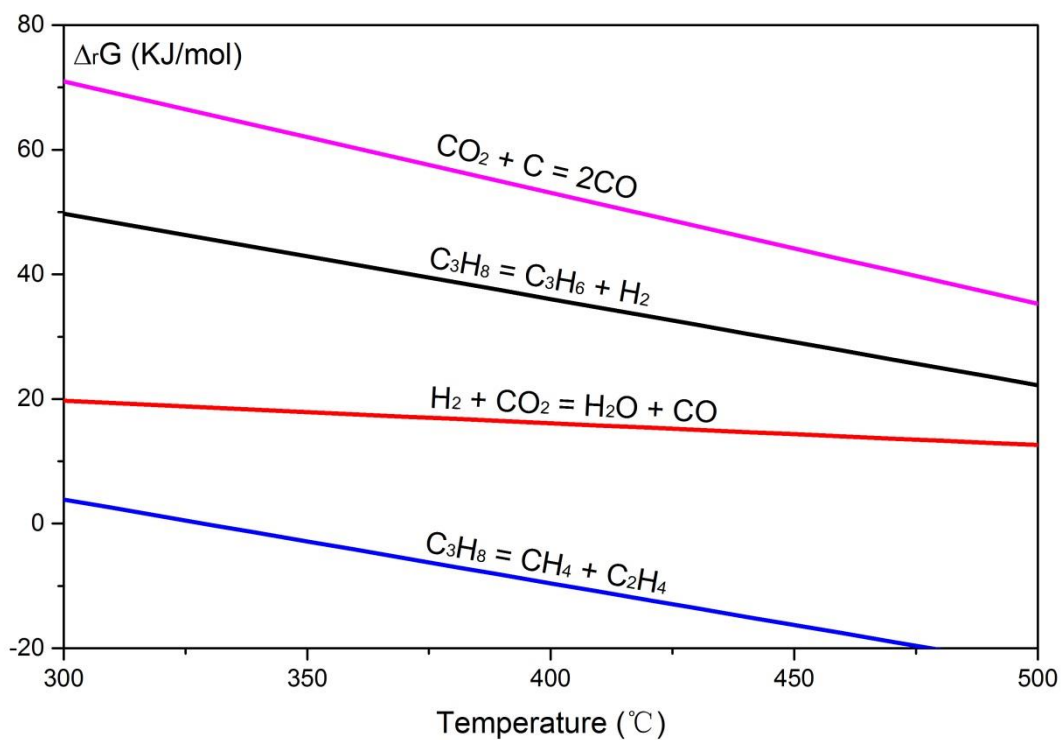


Figure 5 $\Delta_r G_m^\ominus$ of reaction (1), (2), (3), (5) in the modelled system, at 300-500 $^\circ\text{C}$.

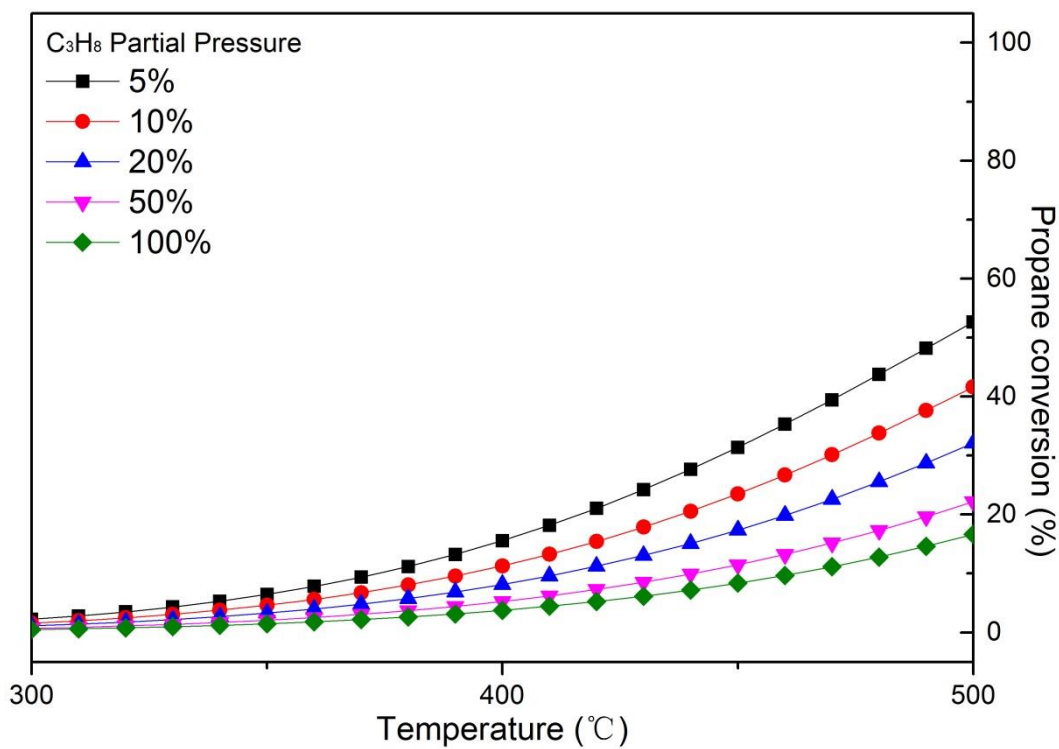


Figure 6 Calculated C_3H_8 conversions (mole %) at equilibrium state, considering reaction (1) only; various C_3H_8 partial pressure; 300-500 $^\circ\text{C}$.

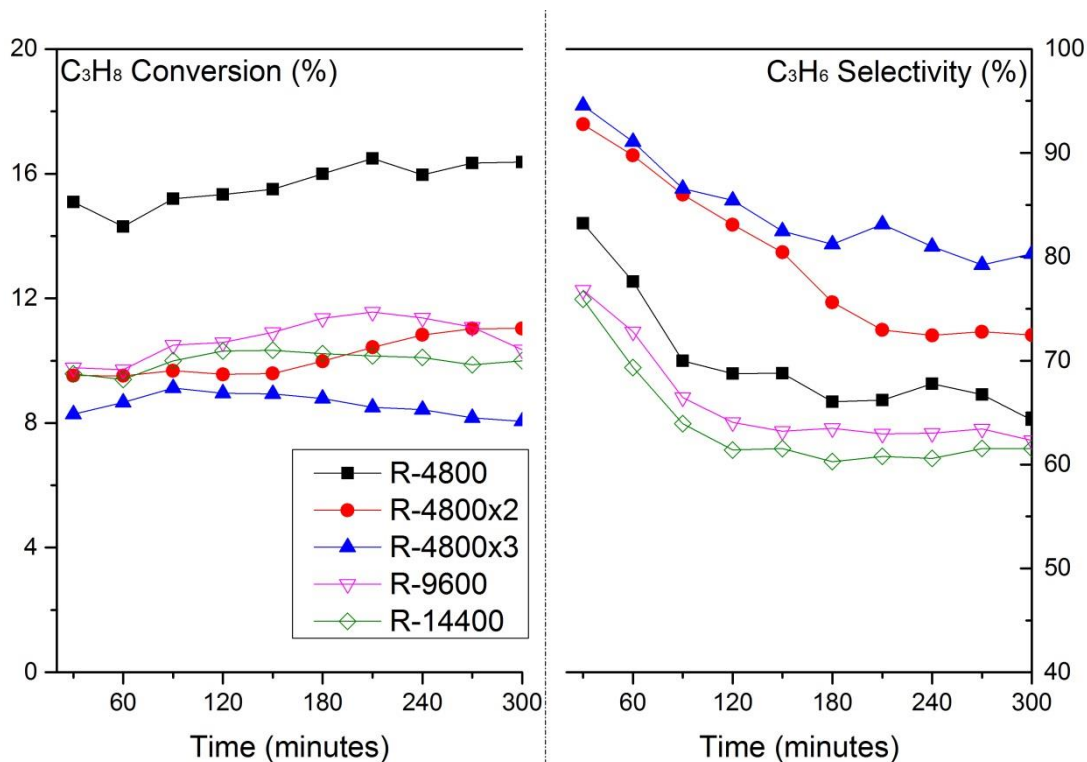


Figure 7 C₃H₈ conversion and C₃H₆ selectivity over 5wt%-Cr₂O₃/ZrO₂ upon operation time at various C₃H₈ partial pressure and overall GHSV; 500°C and C₃H₈/CO₂ = 0.5.

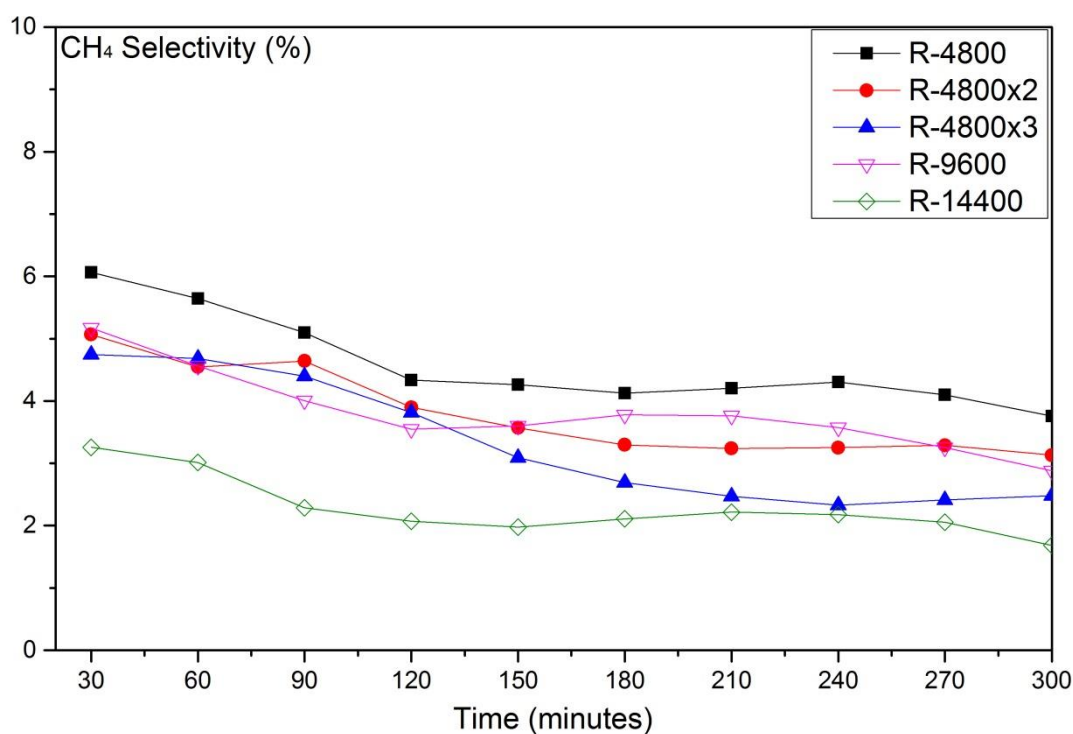


Figure 8 Dependence of the CH₄ selectivity with time on stream over 5wt%-Cr₂O₃/ZrO₂ at various C₃H₈ partial pressure and overall GHSV; 500°C and C₃H₈/CO₂ = 0.5.

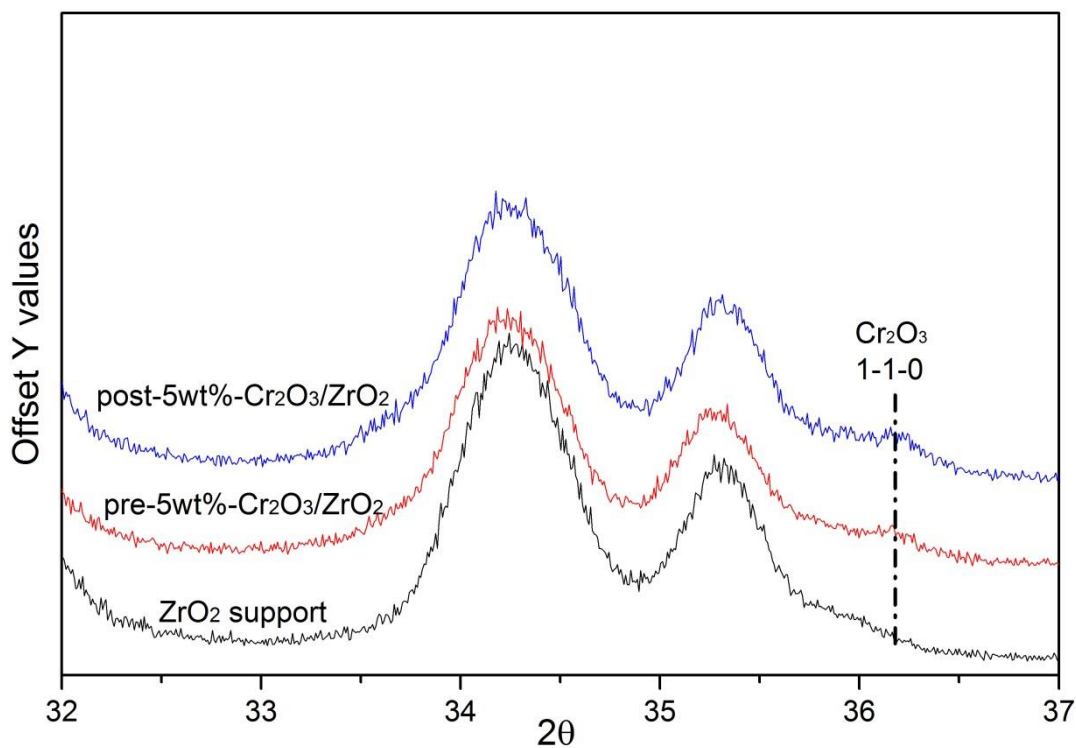


Figure 9 X-ray Diffraction (XRD) results over the catalysts both before (pre-5wt%-Cr₂O₃/ZrO₂) and after (post-5wt%-Cr₂O₃/ZrO₂) the catalytic tests, with ZrO₂ support as reference.

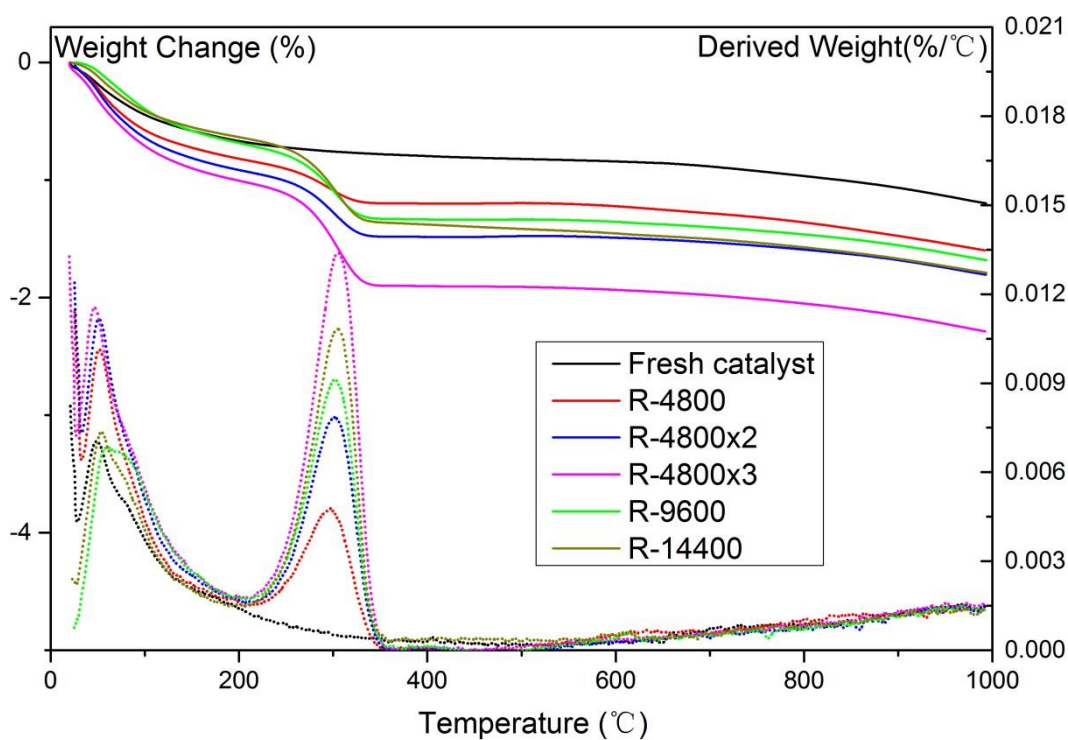


Figure 10 TGA (solid lines) and D-TGA (dot lines) results over 5wt%-Cr₂O₃/ZrO₂ at various C₃H₈ partial pressure and overall GHSV; 500°C and C₃H₈/CO₂ = 0.5.